

Fault Detection and Diagnosis of Broken Bar Problem in Induction Motors Base Wavelet Analysis and EMD Method: Case Study of Mobarakeh Steel Company in Iran

M. Ahmadi, M. Kafil, H. Ebrahimi

Abstract—Nowadays, induction motors have a significant role in industries. Condition monitoring (CM) of this equipment has gained a remarkable importance during recent years due to huge production losses, substantial imposed costs and increases in vulnerability, risk, and uncertainty levels. Motor current signature analysis (MCSA) is one of the most important techniques in CM. This method can be used for rotor broken bars detection. Signal processing methods such as Fast Fourier transformation (FFT), Wavelet transformation and Empirical Mode Decomposition (EMD) are used for analyzing MCSA output data. In this study, these signal processing methods are used for broken bar problem detection of Mobarakeh steel company induction motors. Based on wavelet transformation method, an index for fault detection, CF, is introduced which is the variation of maximum to the mean of wavelet transformation coefficients. We find that, in the broken bar condition, the amount of CF factor is greater than the healthy condition. Based on EMD method, the energy of intrinsic mode functions (IMF) is calculated and finds that when motor bars become broken the energy of IMFs increases.

Keywords—Broken bar, condition monitoring, diagnostics, empirical mode decomposition, Fourier transform, wavelet transform.

I. INTRODUCTION

ELECTRICAL motors are an integral part of the industrial unit and play an important role in efficient vehicle and industrial processes. Especially the squirrel cage electric motors are known as the horse industry. Therefore, recognizing the diagnosis fault of these motors can have many economic benefits [1].

About 80% of the stimuli in the industry are induction motors. Today, due to the high cost of this equipment as well as high repair costs also due to financial losses due to unplanned cessation of production lines, their care and maintenance is very helpful. The widespread use of this type of machine has led to extensive research in the area of troubleshooting. The broken of rotor bars is a common fault that occurs in rotor of squirrel cage of motors. About ten percent of the defects of these motors are included. Fault detection of the rotor broken bars through the waveform of the motor current flow is very difficult. In the past, methods such

M. Ahmadi is with the Technical Inspection Office, Mobarakeh Steel Company, Isfahan, Iran (corresponding author, phone: +989132868779; e-mail: mehdi_a346@yahoo.com).

M. Kafil and H. Ebrahimi are with the Technical Inspection Office, Mobarakeh Steel Company, Isfahan, Iran.

as FFT and Short Fast Fourier Transform (SFFT) were used for ease of diagnosis. Recently, the use of wavelet transformation and the EMD method of signal has also become commonplace [2].

II. MEASUREMENT METHOD

The signal used in this paper, are provided by a current measurement device by 4 kHz sampling frequency, sampled one of the motors of the fan processing unit of Mobarakeh Steel Company. The study was based on the motor's current signals from when the motor was healthy until it was done with the passage of time due to the operation of the truncated motor and the broken of the rotor bars. The reason for using this equipment is that during the measurements, the load of this motor is almost constant, and the motor is working almost equally with a constant speed and slip.

The name plate of this motor is as follows: The nominal power = 1800 kW, nominal voltage = 6/6 kV, nominal current = 184 A, nominal speed = 985 RPM and power frequency = 50 Hz. It is noteworthy that the Current Transformer (CT) conversion ratio is not included in the measurement.



Fig. 1 Motor of fan process

III. DETECTION OF THE BROKEN OF THE ROTOR BAR BASED ON THE FREQUENCY COMPONENT

In normal motor operation, if one of the rotor bars is cracked or broken, because of the asymmetry, a right turn field and a left turn field in the rotor are formed at a speed rate $\pm S f_s$ (S is slip of motor and f is motor input frequency) [3], [4]. Given that the speed of the rotor's field is equal to the

stator $(1-S)f_s$, therefore, the flow frequency induced in the rotor via left turn field is equal to (1).

$$(1-S)f_s - S f_s = (1-2S)f_s \quad (1)$$

Due to the interaction between the rotor's left turn field and the main field of stator, the angular momentum of the torque equals $2Sf_s$. Due to the slippery nature of the phenomenon of frequency modulation in the rotor, the frequency of the $f_{RB} = (1 \pm 2S) \times f_s$, in the rotor comes into existence [5]-[7]. In the above relation, f_{RB} is the frequency of the rotor broken bar.

IV. THEORY OF FOURIER ANALYSIS

The art spent on Fourier transform is that a function or a time waveform can be implemented with a weighted sum of several sinusoidal functions. In fact, a time function can be written as the following:

$$f(t) = \sum_{n=0}^{\infty} W_n \cdot \sin\left(\frac{2\pi \times n \times f_0}{T} t\right) \quad (2)$$

W_n means the corresponding sinus contribution in the form of the function of $f(t)$. Or better, it can be said that W_n is the contribution of $n \times f_0$'s frequency to the desired function for $n = 1$ to infinity. So, the output of the Fourier transform is a set of amplitudes and frequencies.

V. CURRENT SIGNAL ANALYSIS BY FOURIER TRANSFORM

The signals obtained from the motor are listed in two modes when the motor is completely healthy and when the motor becomes faulty over time is shown in the following figures.

The condition of the motor is broken of rotor bar, the waveform and frequency spectrum of the motor current are as:

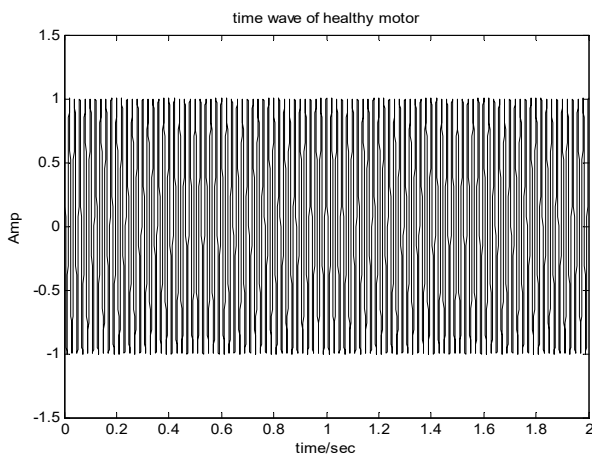


Fig. 2 Time wave of healthy motor

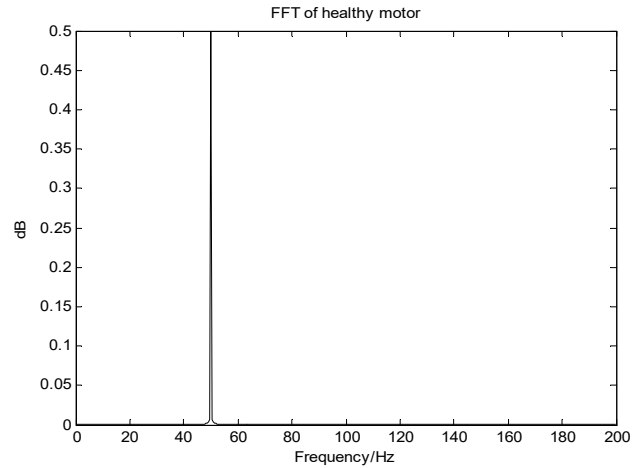


Fig. 3 Spectrum of healthy motor

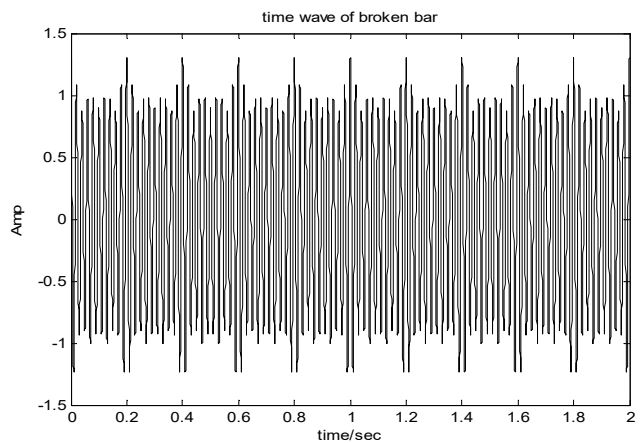


Fig. 4 Time wave of motor by broken bar

VI. THEORY OF WAVELET TRANSFORM

To make multi-resolution transitions, wavelet transformation or wavelet analysis is used that is a customizable window-handling technique [8], [9].

The wavelet transform delivers a time representation. The frequency of the signal has two important characteristics. Firstly, the optimal resolution of the signal is given in two areas of time and frequency. This transformation can be represented by convolution $x(t)$ in accordance with (3) and the wavelet function $\psi a, b(t)$.

$$W_{\psi} X(a, b) = \langle X(t) * \psi_{a,b}(t) \rangle \quad (3)$$

where a and b are the scale and transmission parameters respectively. Also, the wavelet function is discretized according to (4).

$$\psi_{j,k}(t) = a_0^{-j/2} \psi(a^{-j} t - kb_0) \quad (4)$$

j and k are correct values and $\psi_{j,k}(t)$ is the base of the discrete wavelet transform.

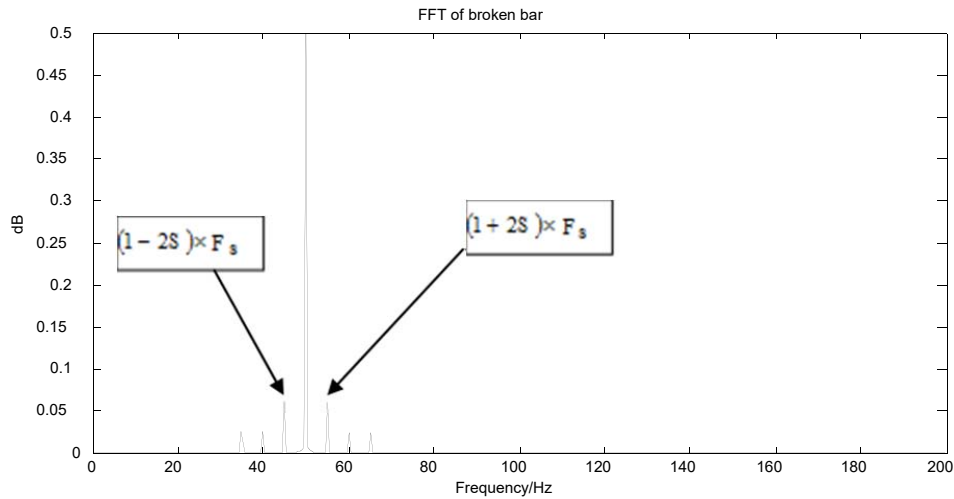


Fig. 5 Frequency spectrum of motor by broken bar

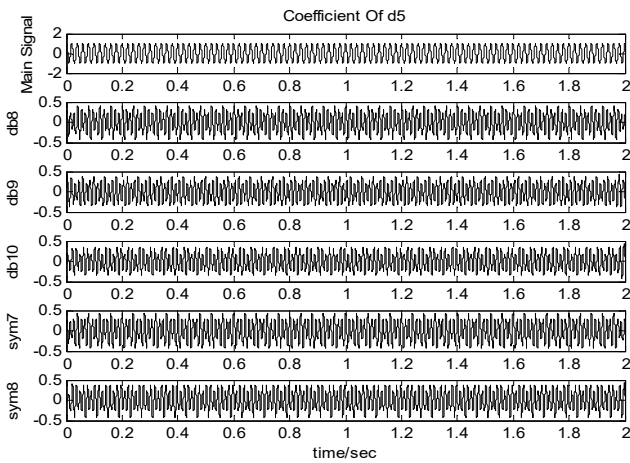


Fig. 6 Details of the signal coefficients of healthy motor

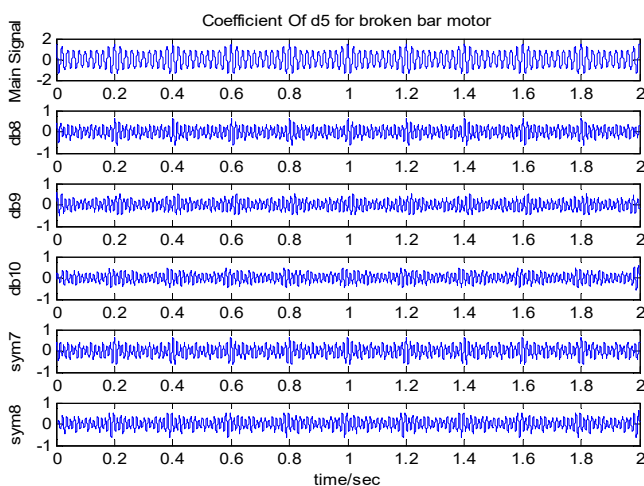


Fig. 7 Details of the signal coefficients of motor by broken bar

VII. USING FROM THE DETAILS OF SIGNAL

By applying the DWT conversion to the MATLAB software on the signals obtained the current measurement device can be used to analyze the signal into several frequency bands. Each stage of the analysis consists of two sections of

approximation and details. This frequency-division analysis can be considered as passing the signal of low-pass and high-pass filters in the time domain.

The fact that the highest frequency in the signal is half the sampling frequency, the number of decomposition steps in this research is seven steps. MATLAB2012a software and wavemenu software are used to analyze the signal. Also, mother wavelets have been used from db8 to db10 and sym7 to sym8. Due to the sampling frequency of the flow measurement device is 4 kHz, the use of signal detail coefficients in the fifth (5th) step is appropriate. Also, at this step, we used from the healthy mode and faulty mode of motor. The results are shown in Figs. 6 and 7.

VIII. INTRODUCING AN INDEX FOR FAULT DETECTION

By numerical analysis of parameters such as the effective value of the flow coefficients and the mean change of the points of maximum coefficients and average coefficients, we conclude that with the failure of the broken bars, these parameters also change. So, we introduce a coefficient of identification, that we have shown with CF, to check the changes from the healthy motor stage and the various stages of the defect of the rotor broken bars and defect growth. And the results are presented in Tables I, II [10].

$$CF = \frac{\text{variation of max coefficients}}{\text{Mean coefficients}} \quad (5)$$

The resulting graph of the indexes is shown at Fig. 8. In the figure, we see the variation tracks in two graphs (the upper graph is related to the state that occurred in the broken bar motor and the bottom figure is related to the state of the was healthy). The same was true when the defect occurred in the motor.

IX. THEORY OF EMD

The experimental method for decomposing the signal into its frequency components (EMD) was first presented by

Huang in 1998 [11]. Using this method, we can divide a signal that has several frequency components into its frequency components.

TABLE I
 INDEX OF FAULT DETECTION IN VARIOUS WAVELET FOR HEALTHY MODE

Wavelets	Variation of coefficient	Mean	CF
db8	0.2292	0.2001	1.1454
db9	0.2157	0.1897	1.1370
db10	0.2017	0.1777	1.1350
sym7	0.2459	0.2142	1.1479
sym8	0.2302	0.2012	1.1441

TABLE II
 INDEX OF FAULT DETECTION IN VARIOUS WAVELET FOR BROKEN BAR MODE

Wavelets	Variation of coefficient	Mean	CF
db8	0.2374	0.2016	1.1775
db9	0.2218	0.1909	1.1618
db10	0.2077	0.1789	1.1609
sym7	0.2541	0.2155	1.1791
sym8	0.2369	0.2020	1.1727

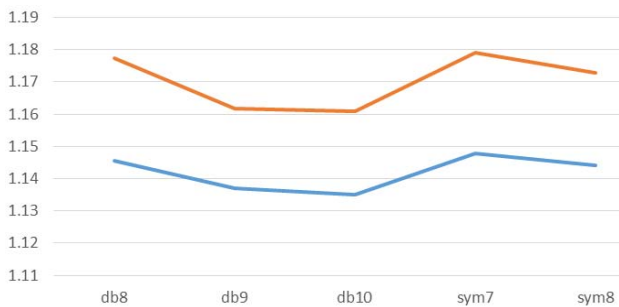


Fig. 8 Index of fault detection (CF), in healthy & broken bar modes

The different steps of this algorithm are described below:
 Step 1: Set the maximum and minimum points of the input signal.
 Step 2: Create a top curve by fitting a grade 3 curve to the local maximum points.
 Step 3: Create a lower curve by fitting a 3rd degree curve over the local minimum points.
 Step 4: Averaging the upper- and lower-case curves.
 Step 5: Subtract the average curve from the input signal according to:

$$h_1(t) = x(t) - m_1(t) \quad (6)$$

Step 6: Check the conditions of the IMF and the conditions of the stop according to:

$$D_k = \frac{\sum_{t=0}^T |h_1^{k-1}(t) - h_1^k(t)|^2}{\sum_{t=0}^T |h_1^{k-1}(t)|^2} \quad (7)$$

Step 7: If the sixth condition is not met, the signal is placed from the fifth step instead of the main signal and the process

continues from the first step.

Step 8: If the condition of the sixth step is present, the process is screened then, $C_1 = h_1^K$, It is considered as the first IMF, which is in fact the high-frequency component of the input signal $x(t)$.

Step 9: The remainder is defined as: $r_1 = x(t) - C_1^K$, And if it fulfills the IMF's condition, it is considered an IMF.

Otherwise, it will be considered as a primary signal, and steps 1 to 4 will be repeated.

In the end, we can say that the main signal is the result of the total IMF and margin.

$$x(t) = r + \sum_{n=1}^N h_n \quad (8)$$

X. SIGNAL ANALYSIS BY EMD METHOD

We were applied EMD method on the four signals. First signal is related to healthy mode. Second signal is related at the start of failure. The third signal is related to when one of the rotor bar is broken, and finally the fourth signal is related to when two rotor bars has been broken. And we used from IMF2 until IMF4 for our studies. The results are shown in Figs. 9-12.

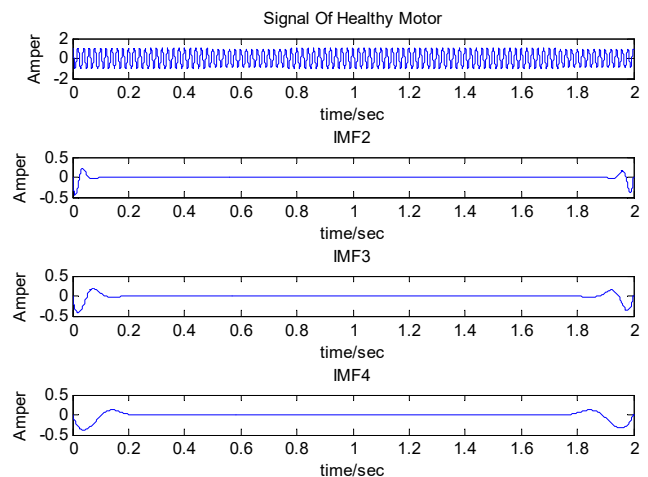


Fig. 9 Main signal and IMF2-IMF4 of healthy motor

XI. INTRODUCTION AN INDEX FOR FAULT DETECTION

We obtained the following results by studying four different modes and numerical analysis on the energy of signals from IMF2 until IMF4. The results are shown in Table III and Fig. 13.

TABLE III
 ENERGY OF IMFS FOR DIFFERENT MODES

IMFs	Healthy mode	Initial of disturbance	One broken bar	Two broken bars
IMF2	4.75	4.78	5.01	5.21
IMF3	6.34	6.41	6.76	6.98
IMF4	7.75	7.80	8.52	8.81

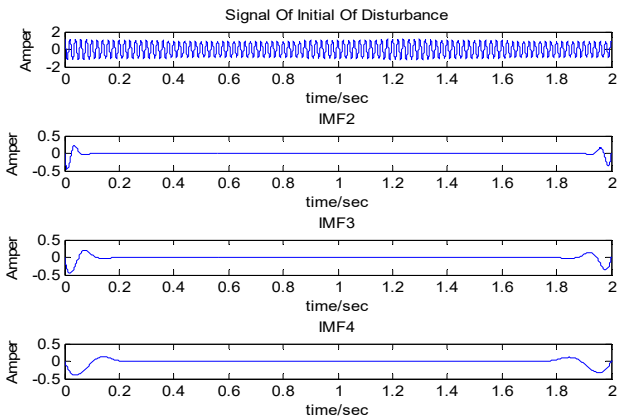


Fig. 10 Main signal and IMF2-IMF4 of initial of disturbance

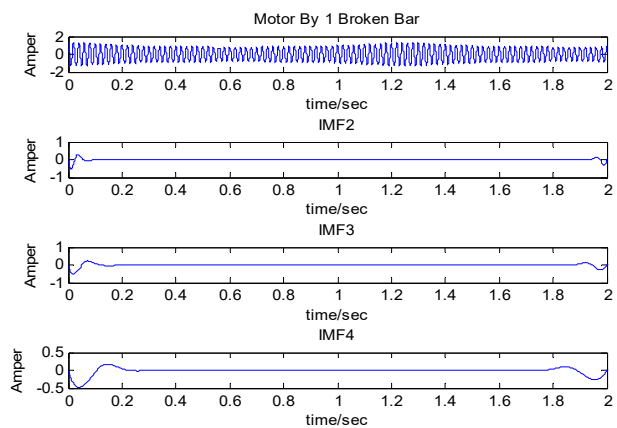


Fig. 11 Main signal and IMF2-IMF4 of one broken bar

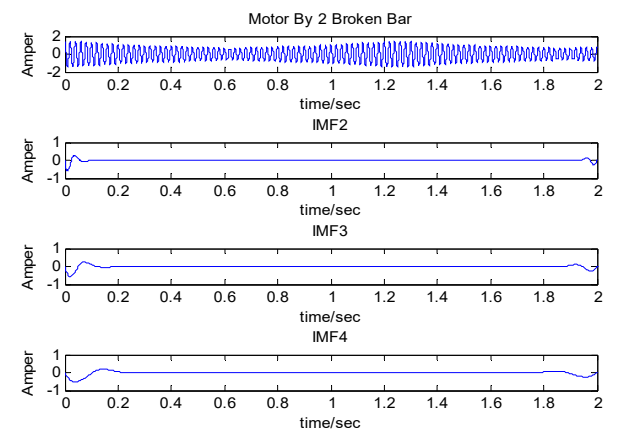


Fig. 12 Main signal and IMF2-IMF4 of two broken bars

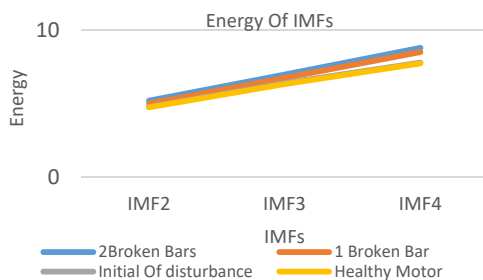


Fig. 13 Chart of energy of IMFs

XII. CONCLUSION

Regarding the frequency spectrum obtained in two modes of a healthy motor and defective motor, the broken of the rotor bars in the motor was determined. Also, with the help of wavelet analysis, and chart given according to Tables I and II and Fig. 8, it can be concluded that the rotor bars are broken and defective. The index factor (CF) is greater than that of a healthy motor. And this can be a suitable index for detecting fault in the rotor bars failure in the motors. Also, with the help of EMD analysis, considering four different motor modes, when the motor was healthy and when two of its rotor bars were broken, and according to Table III and Fig. 13, we can conclude that the energy generated by the IMF signal has grown in the event that the motor starts to fail and when it goes to broken bar mode.

ACKNOWLEDGMENT

The authors would like to deeply thank the *Rotary Machinery and Power Equipment Technical Inspection Office*, and *Power Distribution Plant at Mobarakeh Steel Company, Isfahan, Iran*; for provision of information, technical infrastructure and access to the required data.

REFERENCES

- [1] Austin H. Bonnet; George G. Soukup, "Cause and analysis of stator and rotor failures in 3 phase squirrel cage induction motors" IEEE trans-on Industry application vol 28, no. 7, July 2003, pp 921-237.
- [2] G. Eason, B. Noble, and I.N. Sneddon, "On certain integrals of Lipschitz-Hankel type involving products of Bessel functions," Phil. Trans. Roy. Soc. London, vol. A247, pp. 529-551, April 1955.
- [3] Yavanda and Bhim Singh "Identification of Three Phase Induction Motor Incipient Faults "19-22 September 2004.
- [4] Ricardo Carvalho J. O. "Dynamic Performance of Induction Motor Under Non Sinusoidal Condition"2002IEEE.
- [5] A. Bellini, F. Filippetti, G. Franceschini, C. Tassoni, and G. B. Kilman, "Quantitative evaluation of induction motor broken bars by means of electrical signature analysis," IEEE Trans. Industry Applications, vol. 37, no. 5, pp. 1248-1255, Sep/Oct 2001.
- [6] J. Faiz, and B. M. Ebrahimi, "Determination of number of rotor broken bars and static eccentricity degree in induction motor under mixed fault," Electromagnetics, vol. 28, no. 6, pp. 433-449, August 2008.
- [7] G. Didier, E. Ternisien, O. Caspary, and H. Razik, "Fault detection of broken rotor bars in induction motor using a global fault index," IEEE Trans. Ind. Appl., vol. 42, no. 1, pp. 79-88, Jan./Feb. 2006.
- [8] Riera-Guasp, M, et al., "A General Approach for the Transient Detection of Slip -Dependent Fault Components Based on the Discrete Wavelet Transform," IEEE Transactions on Industrial Electronics, vol. 55, no. 12, pp. 4167-4180, 2008.
- [9] Siau, J, et al., "Broken Bar Detection in Induction Motors using, New Zealand, 2003.
- [10] S. M. Shashidhara "Tradeoff Analysis of Wavelet Transform Techniques for the Detection of Broken Rotor Bars in Induction Motors" © Research India Publications, Advance in Electronic and Electric Engineering. ISSN 2231-1297, Volume 3, Number 8 (2013), pp. 1019-1030.
- [11] Norden E. Huang, Zheng Shen, Steven R. Long, Manli C. Wu, Hsing H. Shih, Quanan Zheng," The empirical mode decomposition and the Hilbert spectrum for nonlinear and non-stationary time series analysis" Published 8 March 1998.DOI: 10.1098/rspa.1998.0193.